SMiRT–12 / K. Kussmaul (Editor)
1993 Elsevier Science Publishers B.V.

BG10/2

EFFECT OF CRACK DEPTH ON CRACK TIP STRESS FIELD AND CRACK INITIATION

K. Ikonen and H. Raiko

Technical Research Centre of Finland, Nuclear Engineering Laboratory, P.O. Box 208, SF-02151 Espoo, Finland

ABSTRACT

Numerical results of the shallow crack effect is presented. The fracture toughness in transition area measured in J-integral is considerably increased, when crack depth or length is low. This phenomenon can be simulated using materially nonlinear FE-method and very detailed FE-mesh to get the actual value of the local stress close to the crack tip region. The cleavage fracture is assumed to take place when the maximum crack closing stress component has reached the critical value. This is, in principle, application of maybe the eldest strength hypothesis in the world, the maximum principal stress hypothesis instead of J-integral approach. The result of these kind of analyses can be used as a constraint correction parameters in fracture toughness experiments, where the specimen dimensions (size) do not fulfil the requirements to produce small scale yielding (SSY) condition. Even the very largest test specimen do not exactly produce the SSY condition, so, a numerical analysis of this kind always decreases the amount of error in test result interpretation.

1 INTRODUCTION

When making fracture mechanics tests with small or moderate size test specimen, the K_I-dominated stress field is highly disturbed in 2D-specimens close to free surfaces or in all the crack area, if the crack is shallow or ligament is small compared to other dimensions of the small specimen. All these effects are increased in significance if the plastic zone in the crack tip is large compared to the depth (a) or ligament of the crack, ref. [*Anderson*], [*Dodds & al*]. The code requirements (ASTM E399-83 and ASTM E813-87) define the minimum size of the test specimen as a function of flow stress and J-integral loading level. However, to know more exactly the 3D-stress state, the effect of reduced constraint at or close to free surfaces, the form and width of plastic zone, the variation of COD and J-integral in the front of crack tip, and the possible errors in interpretation of test measurements, very detailed nonlinear 3D-FEM-analysis is needed. In the following, a short description of the FE-analysis system made for this kind of analysis is given and some numerical results are reported and discussed. The results show that a lot of error can be avoided in the interpretation of fracture mechanics test results, if a detailed 3D FE-analysis is made in addition to the test itself with known stress-strain-relationship of the tested material and known shape and dimensions of the test specimen and initial crack.

2 STRESS FIELDS IN CLEAVAGE FRACTURE

If we look at stress components in front of crack tip in mathematical plane strain (MPS) condition, Fig.1, we can see that the crack closing stress component in the very tip of the crack is equal to yield strength corresponding the strain rate. This means that the stress state at the blunted crack tip is two dimensional due to the free surface of the blunted crack tip. If we go ahead of the tip, the stress state becomes more three dimensional and the current stress components become much higher. The maximum of crack closing stress component is about three times yield stress and the location of the maximum is about 2 - 4 times CTOD in front of the tip. This can be decided even by linear elastic reasoning, by FEM or by slip line theory.

The cleavage fracture is assumed to take place when the maximum crack closing stress component has reached the critical value. This is, at least in principle, application of the eldest strength hypothesis in the world, the maximum principal stress hypothesis by Rankine, Lamé, Clapeyron and Maxwell. Keeping this in mind, we can make a correlation between the measured value of critical J-integral from a test specimen and the respective critical J-integral value in undisturbed small scale yielding field, (SSY). This kind of application can be used in the lower transition region where extensive plasticity precedes unstable fracture.

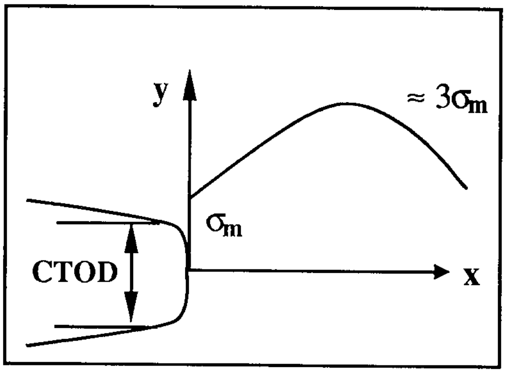

Figure 1. *The maximum crack closing stress component in front of a crack tip.*

3 NUMERICAL ANALYSIS PROCEDURE

A FE-method based computer code was developed for special analysis purpose now in question. The basis of the program is a typical materially nonlinear FE-program. The nonlinear behavior of material is programmed according to von Mises's yielding condition and associative flow rule [*Hill*]. Due to nonlinearities the analysis process is incremental and step by step iterative. The special features needed in nonlinear analysis of stress fields very close to crack tip are:

- automatic node and element generation for very high density, well shaped and balanced mesh in the crack tip area,
- calculation of CTOD according to [*Shih*] in the crack front during the incremental analysis,
- calculation of J-integral in the crack front by path and domain integral method,
- calculation of maximum crack closing stress component (the most positive principal stress component) in front of crack tip in the distance of about 1 to 10 CTODs during the incremental analysis,
- automatic reference case analysis (small scale yielding), where the FE-modeled crack tip area is analyzed with forced displacement boundary conditions based on analytical solution of small scale yielding infinite field [*Dodds & al*], which gives a HRR-field close to crack tip, ref. [*Hutchinson*], [*Rice & Rosengren*], and
- comparison of calculated J-integral values in small scale yielding field solution and real test specimen geometry solution corresponding to equal maximum crack closing stress

component in front of the crack front locating in the distance of about 2 - 4 times local CTOD, ref. [*Dodds & al*].

First a 2D FE-program was developed including the features described above. The 2D program includes the options of analyzing plane strain, plane stress and axisymmetric stress state. After doing a lot of 2D analysis it became evident that in addition to the relative shallowness (a/W) of the crack the distance of free surface at the ends of the crack in specimen geometry also had a prominent effect in local stiffness, stresses and J-integral values. Therefore, the FE-code was expanded into 3D. In 3D program the calculation of J-integral had to be changed from line integral to domain integral method. The 3D program is able to model the effect of the partly plain stress state close to free boundary at the specimen edge. Accordingly, the possible side grooves of the specimen can be exactly modeled in the analysis. The 3D analysis gives the maximum J-value in the middle of the specimen and the average J-value over the crack front can be calculated, too. Thus we are able to compare the measured average value and the real maximum value of fracture parameter. The need of very small elements, whose dimensions are equal to order of CTOD, and the need of calculating high stresses compared to uniaxial yield strength causes frequently some numerical troubles and the iteration processes have to be continued to very high accuracy to get stable results. The updating of stiffness matrix is important for accurate and effective calculation. The code arithmetics is done in 64 bit accuracy.

4 MODELING OF THE CRACK TIP

In 2D analysis 8-noded and in 3D analysis 20-noded isoparametric elements with reduced or full Gauss quadrature were employed in the models. The mesh close to crack tip front is generated in polar coordinate system. The mesh is usually generated only for a symmetric half of the structure. Circumferentially the elements are evenly distributed typically in 8 or 12 element sectors. Radially the elements are generated so that the radial dimension of the element layer is increasing in geometric series. The minimum element size close to the crack tip must be order of one COD with reasonable load level and the outside diameter of the circular mesh area must be at least ten times the plastic zone dimension. The reasonable size ratio between radial element layers is between 1 to 2. This leads to 10 to 30 radial layers of elements in the near tip field mesh. These rules yield typically to element meshes shown in Fig. 2. for three point bend specimen. There are 1092 nodes and 329 elements in the mesh. The semi circular area close to crack tip contain 30 layers of 8 elements.

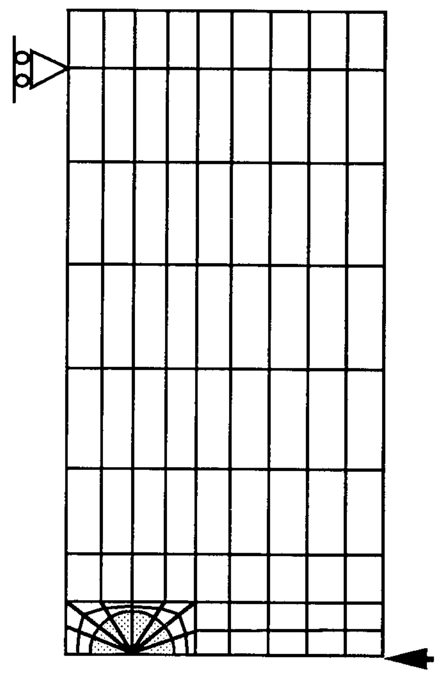

Figure 2. *Typical 2D mesh for three point bend test specimen.*

5 NUMERICAL RESULTS FOR THREE POINT BENDING SPECIMEN

First application of the 2D FE-analysis system was the analysis of a three point bending test specimen (W=150, B=75 and L=600 mm). In some tests the initial crack length had been a=15 mm. The material stress-strain relationship in test temperature was tested and constants for Ramberg-Osgood material model were defined.

First a reference analysis was made for the SSY-solution. A semi circular element mesh with high element density was made. The load for that was a forced displacement field at the outer boundary of the model. The displacement field is based on analytical solution of small scale yielding infinite field. The forced displacement components at radial distance R in angular coordinates θ are as follows:

$$u_x = \frac{(1+\nu)K_I}{E}\sqrt{\frac{R}{2\pi}}\,(3-4\nu-\cos\theta)\,\cos(\theta/2) \tag{1}$$

$$u_y = \frac{(1+\nu)K_I}{E}\sqrt{\frac{R}{2\pi}}\,(3-4\nu-\cos\theta)\,\sin(\theta/2) \tag{2}$$

The SSY reference analysis was run incrementally as far as the required J-integral level was reached. During all load increment level the J-integral, CTOD and the maximum crack closing stress component were calculated and stored.

Then the analysis for the test specimen was done. The element model and mesh was like in Fig. 2. The loading force F was incrementally increased and J-integral, CTOD and maximum crack closing stress component were calculated, respectively. When the maximum crack closing stress component and value of J-integral were compared in SSY analysis and the test specimen analysis, following result was received, Fig. 3. Equal analysis with the same material properties was repeated also for a three point bending test specimen (W=100, B=50 and L=400 mm), and the result is plotted in Fig. 3, too.

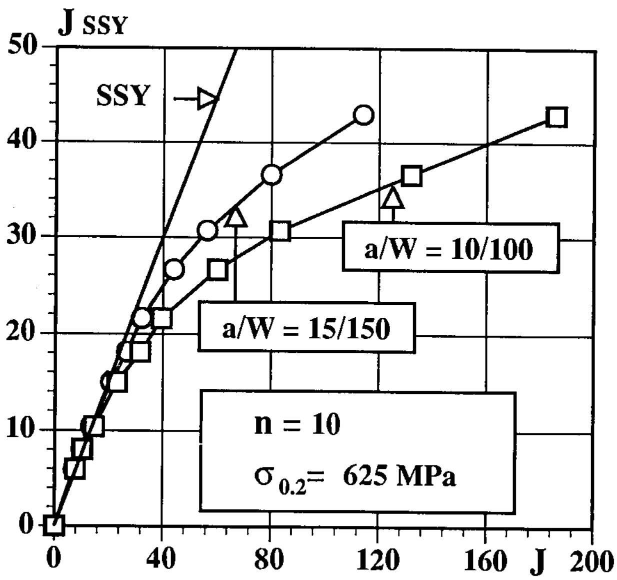

Figure 3. *Relation between J-integral values in test specimen and in SSY condition at loading levels which generate equal maximum crack closing stress component. Parameter n is hardening exponent.*

The result given in Fig. 3 were converted into temperature/stress intensity factor -coordinate system to visualize more clearly, what is the shallow crack effect in this test specimen and material property case. The J-integral values were converted to K_I-parameter values and, moreover, the K_I-parameter values corresponding to SSY condition were calibrated to a typical exponential K_{Ic}-curve. Then the calculated test specimen K_I-result could be plotted in same figure. The result is plotted in Fig. 4. There are also calculated result with the same specimen geometry but a slightly different material properties.

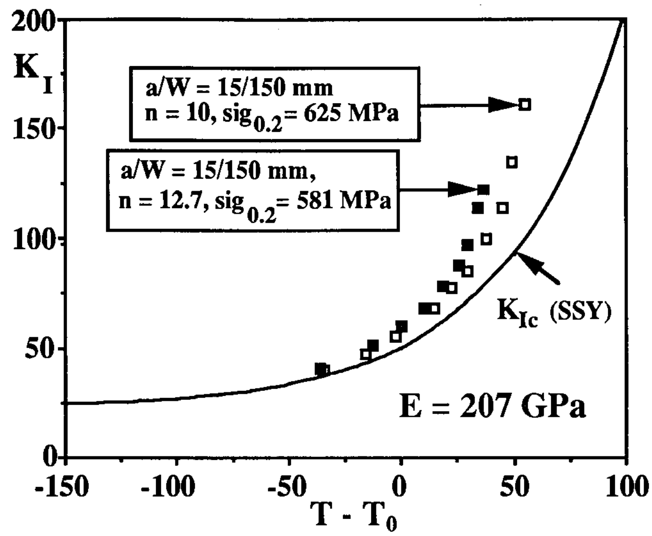

Figure 4. *Test specimen results and the corresponding critical K_{Ic}-values (SSY).*

6 THE CRACK DEPTH CORRELATION TO FRACTURE TOUGHNESS

A primary parameter in the depth effect of the crack is the size of plastic zone compared to the depth of the crack. In the regime of linear fracture mechanics the characteristic radius r_p of the plastic zone [*Broek*] in plane strain condition is

$$r_p \sim \frac{K_I^2}{\sigma_y^2} = \frac{EJ}{(1-\nu^2)\,\sigma_y^2} , \tag{3}$$

where K_I the stress intensity factor, σ_y is the yield strength, E elasticity modulus and ν Poisson's ratio. In considering strain hardening σ_y should be substituted by some other characteristic stress. Let this be the parameter σ_o in the Ramberg-Osgood fitting function. A suitable dimensionless parameter to correlate to fracture constraint is the ratio between the radius r_p and the crack depth a. Thus we can seek the crack depth correlation in form

$$J_c = [1+k\left(\frac{E}{1-\nu^2}\;\frac{J}{a\sigma_0^2}\right)^m]\; J_{cSSY} . \tag{4}$$

This fitting fulfills the requirement $J_c \rightarrow J_{cSSY}$, when $a \rightarrow \infty$. Formally it follows

$$K_{IJc} = \sqrt{1+k\left(\frac{E}{1-\nu^2}\;\frac{J}{a\sigma_0^2}\right)^m}\; K_{Ic} , \tag{5}$$

where K_{IJc} is calculational fracture toughness.

By fitting a curve by least squares in Fig. 4 to the points calculated by FE-method in the interested area, namely below $K_{Ic} \approx 100$ MPa$\sqrt{m}$ values k = 0.993 and m = 0.889 are obtained and equation (5) will look like

$$K_{IJc} = \sqrt{1+0.993\left(\frac{K_{Ic}^2}{a\,\sigma_0^2}\right)^{0.889}}\; K_{Ic} \; . \qquad (6)$$

It should be emphasized that equation (6) is valid only when n = 10. For other hardening modules n the parameters k and m must be calculated accordingly.

CONCLUSION

Numerical application FE-method to correlate test specimen size and hardening material properties to fracture toughness in SSY condition is presented. In addition, a correlation function procedure is proposed to eliminate the shallow crack effect in three point bending specimen.

REFERENCES

Anderson, T. L. 1991. Fracture Mechanics. Boca Raton, FL: CRC Press, Inc.

Broek, D. 1983. Elementary Engineering Fracture Mechanics. The Hague: Martinus Nijhoff Publishers.

Dodds, R. H., Jr., Anderson, T. L. and Kirk, M. T. 1991. A framework to correlate a/W ratio effects on elastic-plastic fracture toughness (J_c). International Journal of Fracture 48: pages 1-22.

Hill, R. 1958. The Mathematical Theory of Plasticity. Oxford: University Press.

Hutchinson, J. W. 1968. Singular Behavior at the End of a Tensile Crack Tip in a Hardening Material. Journal of the Mechanics and Physics of Solids 16: pages 13 - 31.

Rice, J. R. and Rosengren, G. F. 1968. Plane Strain Deformation near a Crack Tip in a Power-Law Hardening Material. Journal of the Mechanics and Physics of Solids 16: pages 1 - 12.

Shih, C. F. 1981. Relationships between the J-integral and crack opening displacement for stationary and extending cracks. Journal of the Mechanics and Physics of Solids 29: pages 305 - 326.